A.N. Ponyavina, E.E. Tselesh, A.D. Zamkovets

Optical Properties of Planar Densely-Packed Plasmonic Nanocomposites

Institute of Physics, National Academy of Sciences of Belarus, Nezavisimosti Ave., 68, Minsk, 220072;
e-mail: a.zamkovets@dragon.bas-net.by

For planar nanocomposites Ag-LiF and Ag-KCl which were fabricated by the thermal vacuum evaporation and characterized by a high volume part of a metal phase (p = 0,4 - 0,8), the concentration features of the surface plasmon absorption band were established and analyzed. Based on the probabilistic approach to the description of a nanocomposite structure, the new combined model of the effective medium is proposed.

Keywords: optical spectra, plasmonic nanocomposites, silver nanoparticles, effective medium approximation

Introduction

Plasmonic nanocomposites are of great importance for novel functional material development. One of the universal and effective methods of plasmonic nanocomposites fabrication is a thermal vacuum evaporation. Changing a metal phase concentration and a composite topology gives opportunities to control a spectral position and intensity of bands corresponding to surface plasmon resonances of absorption (SPRA).

Simulation of ultradisperse composite optical properties is often made with the use of the effective medium approximation (EMA) [1 - 5]. The most famous are Maxwell Garnett (MG) and Bruggeman theories with their own fields of an application. The attempt to combine the MG and Bruggeman theories advantages was made by Sheng [6]. Recently a new simplified combine model of effective medium (CMEM) was proposed for nanocomposites with an arbitrary ratio between volume concentrations of their components [7]. Both the CMEM and the Sheng model are based on a probabilistic approach to a nanocomposite structure description what determines their adaptability in the range of matrix inversion that takes place at comparable concentrations of nanocomposite constituencies. In this paper the CMEM are applied for an analysis of optical characteristics of densely-packed plasmonic nanocomposites which were fabricated at the process of a thermal vacuum evaporation.

I. Experimental procedure

Experimental samples were fabricated by means of a consistence thermal evaporation of silver and a corresponding dielectric (KCl or LiF) at a vacuum on glass and quartz substrates. Pressure of residual gases was 2×10^{-3} Pa. Samples were of a room temperature. Control of layer thicknesses evaporated was made with a use of a quartz sensor. Spectral characteristics of experimental samples under investigation were recorded on the spectrophotometer "Cary 500".

II. Calculation method

In order to regard values of an effective dielectric permittivity ε_{eff} of plasmonic nanocomposites we used both the MG and the CMEM approximations.

The well-known MG expression [1] may be transformed to the following formula, which is more suited for numerical calculations:

$$e_{eff}^{MG} = \frac{2e_0(e - e_0)p + e_0(e + 2e_0)}{(e + 2e_0) - (e - e_0)p}. \qquad (1)$$

Here $e = e' + ie''$ and $e_0 = e'_0 + ie''_0$ – complex dielectric permittivity of grain and matrix materials, respectively.

The CMEM approximation leads to the following formula:

$$e^{CMEM}_{eff} = w_1 \frac{2e_2(e_1-e_2)p_1 + e_2(e_1+2e_2)}{(e_1+2e_2)-(e_1-e_2)p_1} + w_2 \frac{2e_1(e_2-e_1)(1-p_1)+e_1(e_2+2e_1)}{(e_2+2e_1)-(e_2-e_1)(1-p_1)} \qquad (2)$$

Here $w_1 = (1-p_1^{1/3})^3 / [(1-p_1^{1/3})^3 + (1-p_2^{1/3})^3]$, $w_2 = (1-p_2^{1/3})^3 / [(1-p_1^{1/3})^3 + (1-p_2^{1/3})^3]$, p_1 and p_2 – macroscopic volume concentrations of substances 1 and 2 with complex dielectric permittivity e_1 and e_2, respectively.

Formula (2) was obtained in [7] with an assumption that there are finite probabilities of two different types of a composite medium realization at an each local range of a sample. These two types are differed from each other by an inversion of grain and matrix materials. Type 1 is a case when grains of material 1 (dielectric permittivity ε_1) are located in a matrix of material 2 (dielectric permittivity ε_2). Type 2 is an opposite case when grains of material 2 situated in a matrix of material 1. The averaging over these situations appearing with probabilities w_1 and w_2, respectively, leads to the effective dielectric permittivity, defined by (2).

III. Results and discussion

III.1. Simulation of optical constants with the use of the MG and the CMEM approximations.

Calculations of the complex effective indexes of refraction $m_{eff} = n_{eff} - ik_{eff}$ for nanocomposites Ag/KCl and Ag/LiF with different volume content of silver were made on the base of the MG and CMEM approximations in the spectral range 300-800 nm. Figures 1 and 2a show results obtained for Ag/KCl nanocomposites. First of all it is worthwhile to note that for relatively low value of a metal volume concentration p ($p = 0,1 - 0,3$) formulas (1) and (2) give the same results. In both cases there is an
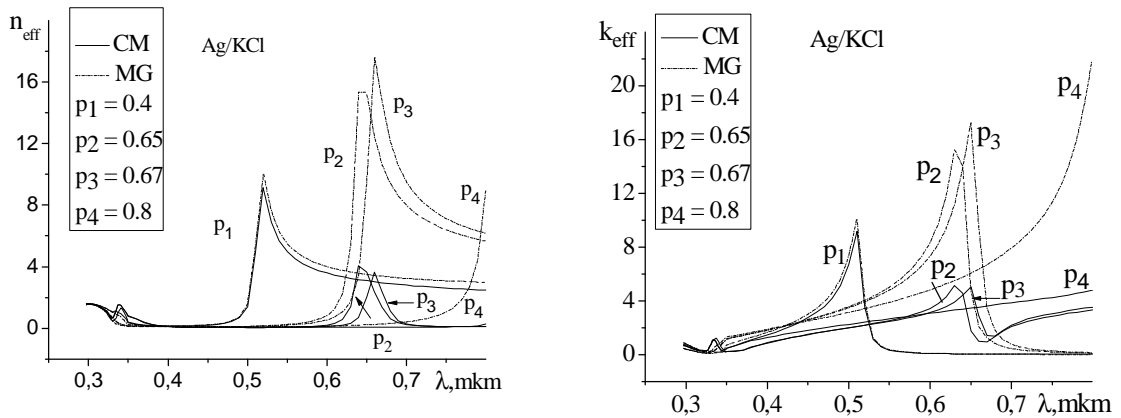
Fig. 1. Spectral dependence of real (a) and imagine (b) parts of an effective index of refraction calculated with the use of the MG (dash lines) and CMEM (solid lines) formulas for Ag /KCl nanocomposites with Ag volume concentrations $p_1 = 0.4$, $p_2 = 0.65$, $p_3 = 0.67$ and $p_4 = 0.8$.
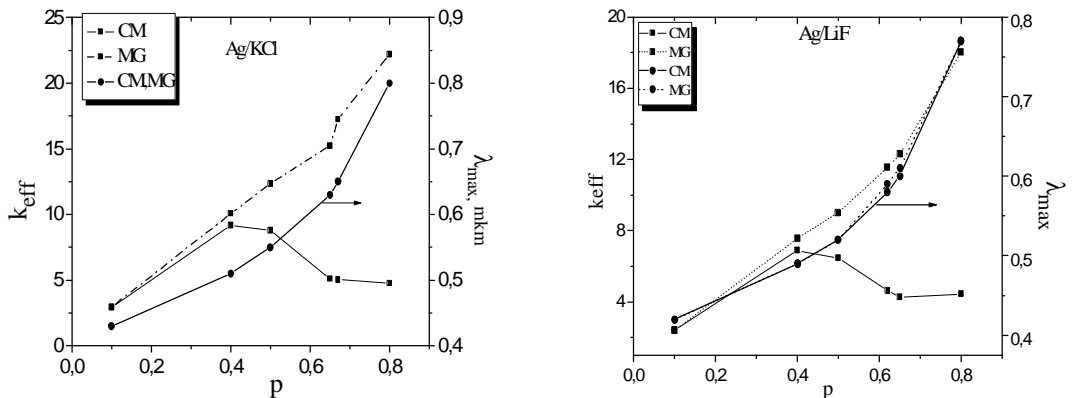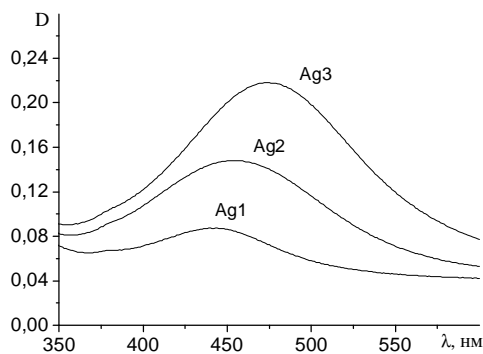

Fig. 2. Concentration dependences of an intensity and wavelength of the SPRA maxima for Ag/KCl (a) and Ag/LiF (b) nanocomposites. Calculations with the use of the MG formula - dash lines, and with the use of the CMEM - solid lines.

absorption band originated from the surface plasmon resonance of silver nanoparticles in the spectral range 450 – 550 nm. With a growth of p this band shifts to a long-wavelength spectral region. However, according to the MG formula the increase of metal volume concentration p gives rise to a monotonic growth of the absorption intensity at the maximum of the band, wherever in the frame of the CMEM approximation one can see its nonmonotonic change. The same features of a concentration dependence of n_{eff} and k_{eff} were also remarked for Ag/LiF nanocomposites (Figure 2,b).

Besides, at the range of a matrix inversion ($p > 0,4$) calculations in the frame of the CMEM demonstrate an appearance of an additional absorption band in the short-wavelength spectral region $\sim 330 – 350$ nm. This weak band originates from a surface plasmon resonance at dielectric nanopores (dielectric inclusions) in a metal matrix. This becomes possible at a high metal concentration, when one can find not only metal nanoparticles surrounded by a dielectric matrix but also dielectric nanovoids, surrounded by a quasisolid metal phase. Nanovoid resonances take place at the condition $2e_{met} = -e_{diel}$ [8]. At the typical Drude frequency dependence of a metal dielectric permittivity the modes of this group are more high-frequency relatively to surface resonances of metal nanoparticles. At the MG model this situation is not taken into account. As a result, qualitative values of n_{eff} and k_{eff} calculated for composites with a high metal concentration ($p > 0,4$) with the use of (1) are uncorrected.

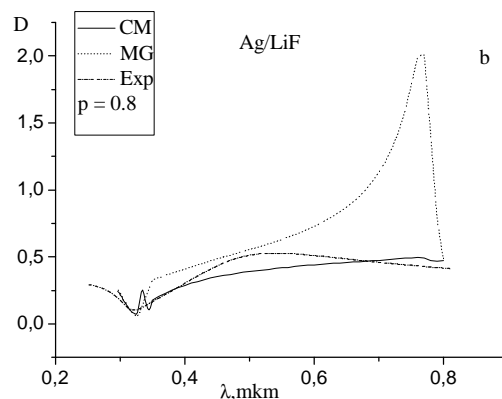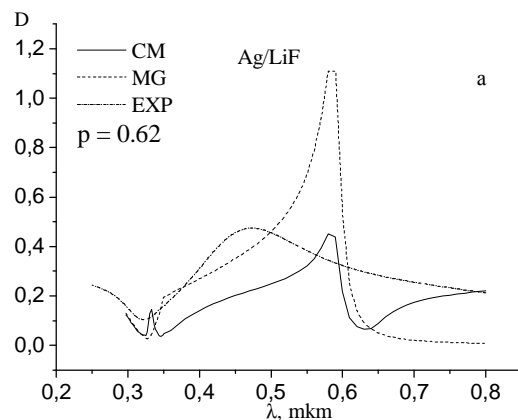### III.2. Optical density of densely-packed plasmonic nanocomposites

At experiment plasmonic nanocomposites were fabricated on the base of densely-packed monolayers of silver nanoparticles. The SPRA of silver nanoparticles is well pronounced because of its significant spectral distance from a region of an interband absorption. Figure 3 demonstrates the optical density spectra of Ag monolayeres with different metal concentration. Maximums of the bands are located in the visible spectral

range and shift to the long-wavelength region at the increase of a metal concentration. At the same time one can see a growth of the band intensity and its half-width. AFM-measurements shown that mean nanoparticle sizes are about $3 – 5$ nm and their density of packing at the largest metal mass (monolayer Ag3) is corresponded to an overlap factor $\eta \sim 0,4 - 0,45$.

In Figures 4 a,b there are optical density spectra of Ag/LiF nanocomposites both fabricated by thermal vacuum evaporation and calculated with the use of the MG and CMEM approximations. Experimental samples of nanocomposites were sandwiches with Ag island films separated by thin LiF interlayers. Nanocomposite 1 consists of four Ag2 monolayers, the first of which contacts with a substrate and the last one is covered by a thin LiF layer. Nanocomposite 2 involves five Ag3 monolayers, the last one bordering with an air. Metal volume concentrations in nanocomposites 1 and 2 were 62 and 80 % , with total thicknesses of 10,4 and 15,7 nm, correspondently. As it can be seen from Figures 4 and 5, at a numerical simulation of the experimental data the fitting is better when one use the CMEM approximation. This concerns both quantitative values of an optical
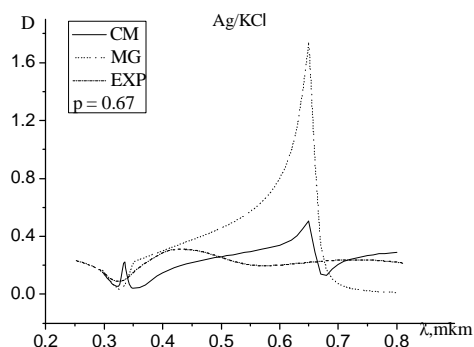
Fig. 3. Optical density of Ag nanoparticle monolayers made by vacuum thermal evaporation. Silver nanoparticle sizes are 3 - 5 nm, surface density of metal is $0,7 \cdot 10^{-6}$ g·sm^{-2} (Ag1); $1,4 \cdot 10^{-6}$ g·sm^{-2} (Ag2); $2 \cdot 10^{-6}$ g·sm^{-2} (Ag3).

Fig. 4. Calculated and measured optical density spectra of the Ag/LiF nanocomposites. Effective thicknesses and volume metal concentrations are correspondingly 10,4 nm and 62 % (a), 15,7 nm and 80 % (б). Fabricated nanocomposite structures are (Ag2/LiF)^4 (a) and (Ag3/LiF)^{4}Ag3 (b).

experimental and calculated spectra of the Ag/LiF nanocomposites. Short-wavelength displacement of the experimental maxima relatively to the calculated one may indicate indirectly on a closing in two SPRA connected both with silver nanoparticles into dielectric matrix and with dielectric voids into metal matrix. Their covering together with other reasons noted above gives rise to a total wide absorption band with a large haft-width.

With the use of thermal vacuum evaporation on glass substrates we also prepared some samples of $(Ag/KCl)^4Ag$ nanocomposites. Their layered periodic structure includes five silver island monolayers separated by four thin KCl films. Metal volume concentrations at nanocomposites were 40 and 67 %, and their total thicknesses were 10 and 12 nm correspondingly. One group of nanocomposites was consisted of the Ag1 monolayeres, whereas other group was based on the Ag2 monolayeres. These nanocomposite spectra are characterized by an existence of two plasmonic resonances in the visible spectral range. These resonances are the most evidence for the $(Ag/KCl)^4Ag$ nanocomposites with a larger metal volume concentration. In the figure 5 spectrum of the optical density of the $(Ag/KCl)^4Ag$ nanocomposite is compared with spectra calculated in the frame of the MG and CMEM approximations. As for the Ag/LiF systems it is evidence that the experimental band intensity and half-width are better described by the CMEM. Existence of two plasmon resonances of absorption in the visible range at measured optical spectra of Ag/KCl nanocomposites may be connected with a number of reasons. Among some main factors are effects of a metal nanoparticle shape, a presence of nanoparticle agglomerates, as well as a role of an air-metal boundary. It must not be ruled out also that one of the absorption bands (short - wavelength) is originated from plasmon resonances at a surface of dielectric voids into a metal matrix.

Conclusion

Structure peculiarities of metal-dielectric nanocomposites fabricated by means of a sequence thermal vacuum evaporation effect strongly on the characteristics of the surface plasmon resonance of absorption that may give additional opportunities to control their optical response.

Fig. 5. Measured (dash-dot line) and calculated with the use of the MG (dash line) and CMEM (solid line) approximations optical density spectra of the Ag/KCl nanocomposite with the effective thickness 12 nm and volume metal concentration 67%. Fabricated nanocomposite structure is $(Ag2/KCl)^4Ag2$.

density at the SPRA maxima and these bands half-widths. It is nevertheless to note that the used theoretical models are based at an assumption about a nanocomposite structure homogeneity including the nanoparticle nearest neighborhood. At the same time at the experiment at any macroscopic packing density (p) the finite probability always exists for a nanoparticle displacement into a local composite environment of a different microscopic density of packing – from 0 till p. This fact effects on the SPRA intensity and half-width leading to a diffusion of the SPRA and it is the most significant at intermediate concentrations at the range of a matrix inversion (p ~ 0,4 - 0,6). This situation is a more characteristic for the nanocomposite 1.

Successive evaporation of metallic and dielectric phases gives rise to a sample stratification, that makes conditions for a conservation of a metal phase dispersiveness at a wider range of a relative metal concentration when compare with a case of a simultaneous evaporation of these two phases. In the own turn a conservation of a metal phase dispersiveness at a concentration higher than 0.5 prevents both from a formation of a short-wavelength plasmonic resonance at the voids into a metal and from the decreasing of a long-wavelength resonance intensity. This principal from the point of a view of a composite topology fact manifests at a very high concentration of a metal phase (p~ 0,6 - 0,8) and effects especially on optical properties of the nanocomposite 2.

One needs also to pay attention to a discrepancy in a spectral position of the absorption band maxima at the

[1] J.C. Maxwell Garnet, Philos. Trans. R. Soc. London. A. 203, 385 (1904).
[2] D.A.G. Bruggeman, Ann. Phys. 24, 636 (1935).
[3] R. Ruppin, Opt. Commun. 182, 273 (2000).
[4] P. Chylek, V. Srivastova, R.G. Pinnick, R.T. Wang, Appl. Opt. 27(12), 1 (1988).
[5] R.J. Gehr, R.W. Boyd, Chem. Mater 8, 1807 (1996).
[6] Ping Sheng, Phys. Rev. Letters 45(1), 60 (1980).
[7] A.N. Ponyavina, S.M. Kachan., and E.E. Tselesh, Journal of Applied Spectr. 79(5), 765 (2012).
[8] C. Bohren and D. Huffman, Absorption and Scattering of Light by Small Particles (Wiley, New York, 1983).